Peptide Nanospheres Self-Assembled from a Modified β-Annulus Peptide of Sesbania Mosaic Virus

Kazunori Matsuura,[1] Yusaku Mizuguchi,[2] Nobuo Kimizuka[2]

[1] *Department of Chemistry and Biotechnology, Graduate School of Engineering, Tottori University, Tottori, Japan.*

[2] *Department of Chemistry and Biochemistry, Graduate School of Engineering, Kyushu University, Fukuoka, Japan.*

Abstract:

A novel β-annulus peptide of Sesbania mosaic virus bearing an FKFE sequence at the C terminus was synthesized, and its self-assembling behavior in water was investigated. Dynamic light scattering and transmission electron microscopy showed that the β-annulus peptide bearing an FKFE sequence self-assembled into approximately 30 nm nanospheres in water at pH 3.8, whereas the β-annulus peptide without the FKFE sequence afforded only irregular aggregates. The peptide nanospheres possessed a definite critical aggregation concentration (CAC = 26 μM), above which the size of nanospheres were nearly unaffected by the peptide concentration. The formation of peptide nanospheres was significantly affected by pH; the peptide did not form any assemblies at pH 2.2 whereas larger aggregates were formed at pH 6.4–11.6.

Keywords: viral capsid, self-assembly, β-annulus peptide, nanosphere

INTRODUCTION

In biological systems, many nanostructures consisting of proteins are formed spontaneously through self-assembly. Spherical viral capsids and clathrin lattices are good examples of natural protein assemblies with a discrete size and they have attracted much attention as biomaterials for nanocarriers.[1-3] Most spherical viral capsids have an icosahedral symmetry and are formed by the self-assembly of multiples of 60 protein subunits.[4] A clathrin lattice is formed by the self-assembly of C_3-symmetric protein subunits (triskelion) in the presence of Mg^{2+} ions.[5, 6]

Recently, chemical strategies for the rational design of artificial proteins and peptides have been progressively developed for the construction of self-assembled nanostructures.[7, 8] Many artificial supramolecular assemblies consisting of coiled-coil α-helix peptides[9-13] and β-sheet-forming peptides[14-19] have been reported. For example, Woolfson and coworkers demonstrated that two complementary coiled-coil bundles self-

assembled into approximately 100 nm unilamellar spheres.[20] Jerala and coworkers developed a folding strategy for the construction of discrete tetrahedral nanostructures with a single-chain coiled-coil peptide.[21] We developed C_3-symmetric, β-sheet-forming peptide conjugates[22-25] and glutathione conjugates,[25-28] which self-assembled into viral-size spherical nanostructures in water.

Tomato bushy stunt virus (TBSV) capsids are formed by the self-assembly of 180 quasi-equivalent protein subunits containing 388 amino acids each and possess a dodecahedral internal skeleton composed of a C_3-symmetric β-annulus motif.[4, 29, 30] We demonstrated that the synthetic 24-mer β-annulus peptide fragment (INHVGGTGGAIMAPVAVTRQLVG) of TBSV spontaneously self-assembled into virus-like nanocapsules in water.[31-34] The β-annulus motif was also found in other spherical viral capsids such as Sesbania mosaic virus (SeMV),[35, 36] desmodium yellow mottle tymovirus,[37] ryegrass mottle virus,[38] cucumber necrosis virus,[39] tobacco necrosis virus,[40] and turnip yellow mosaic virus.[41] SeMV capsids are formed through the self-assembly of 180 quasi-equivalent protein subunits composed of pentameric A and pseudo-hexameric B/C subunits.[35, 36] The β-annulus motif of SeMV consists of a 12-mer peptide (GISMAPSAQGAM) and exists at the center of the C subunit trimer (Figure 1). Herein, we employed a 12-mer β-annulus peptide of SeMV as a novel self-assembling peptide motif for constructing virus-like particles. As the 12-mer β-annulus peptide mainly consists of hydrophobic residues, it was expected that the 12-mer peptide would have poor solubility in water. Thus, we designed a novel β-annulus peptide of SeMV with an FKFE sequence at the C terminus as a self-assembling unit (**1**: GISMAPSAQGMFKFE, Figure 1). In this paper, we report the self-assembling behavior of the 16-mer modified β-annulus peptide of SeMV (**1**) and the 12-mer β-annulus peptide without the FKFE sequence (**2**).

MATERIALS AND METHODS

Reagents were obtained from commercial sources and used without further purification. Reversed-phase HPLC was performed at ambient temperature on a Shimadzu LC-6AD liquid chromatograph equipped with a UV–vis detector (220 nm, Shimadzu SPD-20A) and GL Science Inertsil WP300 C18 (4.6 × 250 mm^2 and 20 × 250 mm^2) columns. MALDI-TOF mass spectra were obtained on an Autoflex III (Bruker Daltonics) spectrometer operated under the linear/positive mode with α-cyano-4-hydroxy cinnamic acid (α-CHCA) as the matrix. CD spectra were collected in a 1 mm quartz cell with a JASCO J-820 spectrophotometer at 25 °C.

Synthesis of peptide 1.

The protected peptide H-Gly-Ile-Ser(tBu)-Met-Ala-Pro-Ser(tBu)-Ala-Gln(Trt)-Gly-Ala-Met-Phe-Lys(Boc)-Phe-Glu(OtBu)-Alko resin was synthesized on an Fmoc-Glu(OtBu)-Alko resin (Fmoc = 9-fluorenylmethoxycarbonyl, Watanabe Chemical Ind., Ltd., 0.51 mmol/g) using Fmoc-based coupling reactions. A solution of 1-[bis(dimethylamino)methylene]-1*H*-1,2,3-triazolo[4,5-b]pyridinium 3-oxid hexafluorophosphate (HATU, 4 equiv) and diisopropylamine (8 equiv) in *N*-methylpyrrolidone (NMP) was used for coupling. A solution of 20% piperidine in *N*,*N*-dimethylformamide (DMF) was used for Fmoc deprotection. The progress of the coupling reaction and Fmoc deprotection was confirmed using a TNBS Test Kit (Tokyo Chemical Industry Co., Ltd.). The peptidyl resin was washed with NMP.

The peptide was deprotected and cleaved from the resin by treatment with a mixture of trifluoroacetic acid (TFA)/water/1,2-ethanedithiol/triisopropylsilane (9.45/0.25/0.25/0.1) at room temperature for 6 h. The cleavage mixture was filtered to remove the resin and the filtrate was concentrated under vacuum. The peptide was precipitated upon addition of methyl *tert*-butyl ether (MTBE) to the residue and the supernatant was decanted. After the peptide was washed three times with MTBE, the precipitated peptide was dried under vacuum. The crude product was purified by reversed-phase HPLC (Inertsil WP300 C18), eluting with a linear gradient of CH_3CN/water containing 0.1% TFA (24/76 to 30/70 over 100 min). The fraction containing the desired peptide was lyophilized to give 1.66 mg of **1** as a flocculent solid (17% yield). MALDI-TOF-MS (matrix: α-CHCA): *m/z* = 1673 $[M + H]^+$, 1711 $[M + K]^+$.

Synthesis of peptide 2.

Peptide **2** (GISMAPSAQGM) was synthesized by nearly the same procedure as described above. This gave a yield of 8.2% for **2**. MALDI-TOF-MS (matrix: α-CHCA): *m/z* = 1121 $[M + H]^+$, 1143 $[M + Na]^+$, 1159 $[M + K]^+$.

Dynamic light scattering (DLS) measurements.

DLS measurements were performed using a Zetasizer NanoZS (MALVERN Instruments, Ltd.) instrument at 25 °C with an incident He−Ne laser (633 nm). During measurement, the count rate (sample-scattering intensity) was also provided. The correlation time for the scattered light intensity ($G(\tau)$) was measured several times and the averaged results were fitted to equation 1:

$$G(\tau) = B + A \exp(-2q^2 D \tau) \quad (1)$$

where B is the baseline, A is the amplitude, q is the scattering vector, τ is the delay time,

and D is the diffusion coefficient. The hydrodynamic radius (R_H) of the scattering particles was calculated using the Stokes−Einstein equation (eq. 2):

$$R_H = \frac{k_B T}{6\pi\eta D} \quad (2)$$

where η is the solvent viscosity, k_B is the Boltzmann constant, and T denotes the absolute temperature.

Transmission electron microscopy (TEM).

A carbon-coated Cu-grid (Oken Co., Ltd.) was hydrophilized for 30 s with a hydrophilization treatment apparatus (JEOL HDT-400). An aliquot (10 μL) of an aqueous solution of peptide **1** was applied to a hydrophilized carbon-coated grid, left for 60 s, and removed. A drop of 2 wt% aqueous ethidium bromide was then placed on the grids. After the sample-loaded carbon-coated grids were dried *in vacuo*, they were observed by TEM (JEOL JEM-2010) using an acceleration voltage of 120 kV.

Scanning electron microscopy (SEM).

An aliquot (10 μL) of an aqueous solution of peptide **1** was applied to a hydrophilized carbon-coated grid, left for 60 s, and removed. The grids were dried *in vacuo* and coated with platinum (3 nm, Hitachi E-1030 ion sputter). The grids were then subjected to SEM observation (Hitachi S-5000) with an acceleration voltage of 15 kV.

RESULTS AND DISCUSSION

Synthesis of modified β-annulus peptide of SeMV

The 16-mer β-annulus peptide of SeMV modified with the β-sheet-forming sequence FKFE (**1**) and the 12-mer β-annulus peptide without the FKFE sequence (**2**) were synthesized by Fmoc solid-phase peptide synthesis in 17% and 8.2% yields, respectively. These peptides were purified by reversed-phase HPLC and confirmed by MALDI-TOF mass spectrometry (**1**: m/z = 1673 $[M + H]^+$; **2**: m/z = 1121 $[M + H]^+$). A lyophilized powder of peptide **1** readily dissolved in deionized water at 3 mM without heating, whereas a lyophilized powder of peptide **2** hardly dissolved in deionized water even at 0.1 mM. Peptide **2** was able to be dissolved in water in the presence of 0.3% 2,2,2-trifluoroethanol (TFE) at 0.1 mM. The poor solubility of **2** in water can be ascribed to the ten hydrophobic and two nonionic hydrophilic residues in the sequence. In contrast, the good solubility of peptide **1** in water can be ascribed to the addition of ionic residues K and E. An aqueous solution of peptide **1** at 0.5 mM had a pH value of 3.8. The CD

spectrum of this solution showed a negative peak at 197 nm and a negative shoulder at approximately 220–240 nm (Figure 2), which is similar to that of the 24-mer β-annulus peptide of TBSV reported previously,[31] indicating the existence of random coils, *β*-structures, and turn structures.

Self-assembly of modified *β*-annulus peptide

The DLS of the aqueous solution of peptide **1** (0.5 mM, pH 3.8) showed the formation of monodispersed assemblies with 32 ± 8 nm hydrodynamic diameters (Figure 3a), which is comparable to that of natural SeMV (30 nm). In contrast, the DLS of the aqueous solution of peptide **2** (0.1 mM containing 0.3% TFE) showed the formation of multidispersed assemblies of 20–400 nm (Figure 3b). TEM (Figure 4a) and SEM (Figure 4c) images of the aqueous solution of peptide **1** also showed the presence of 19–62 nm spherical assemblies. The average diameter of the assemblies was determined to be 33 ± 10 nm, according to the size distribution obtained from the TEM images, which corresponds to the hydrodynamic diameter determined by DLS. Conversely, only irregular aggregates over 1 μm were observed in the SEM image of the aqueous solution of peptide **2** (Figure 4d). Thus, the 12-mer *β*-annulus peptide of SeMV in water self-assembled into irregular aggregates, whereas that of the 16-mer *β*-annulus peptide modified with FKFE self-assembled into closed, viral-size nanospheres. The difference in the self-assembling behavior can be ascribed to the participation of the FKFE sequence, which acts as not only an ionic segment but also a regulation unit for self-assembly. Since the *β*-annulus sequence in C subunit of natural SeMV capsid can form the spherical structure with the assistance of B subunit, it seems that 12-mer *β*-annulus peptide **2** alone could not form spherical structures. It is probable that the peptide **2** might form trigonal *β*-annulus structure, which aggregate due to the hydrophobic character in the aqueous solution.

Effect of concentration and pH on self-assembly

The concentration dependence of the aqueous solution of peptide **1** (pH 3.8) on scattering intensity (Figure 5a) revealed that the CAC at 25 °C is approximately 26 μM, which is comparable to that of the 24-mer *β*-annulus peptide of TBSV in water.[31] Figure 5b shows the concentration dependence of peptide **1** on the hydrodynamic diameter determined by DLS. Similar assemblies of approximately 30–40 nm were observed at concentrations above 0.1 mM, whereas larger assemblies (78 ± 28 nm) were observed at 0.05 mM. At concentrations below CAC (26 μM), DLS autocorrelation data suitable for analysis could not be obtained, indicating minimal assemblies. Therefore, the size of the

assemblies is marginally affected by concentrations above CAC, indicating that 30–40 nm assemblies are stable.

Figure 6 shows the pH dependence of peptide **1** (0.1 mM) on the hydrodynamic diameter determined by DLS. As described above, peptide **1** formed spherical assemblies with 32 ± 8 nm hydrodynamic diameters in aqueous solution at pH 3.8. In contrast, at pH 2.2, the average diameter as determined by DLS was 2.3 ± 0.8 nm, indicating the absence of self-assembled structures. At pH 6.4, 8.2, and 11.6, meanwhile, DLS showed formation of larger assemblies. The pH dependence of the self-assembling behavior of peptide **1** can be ascribed to the difference in peptide charge. From the pK_a values of each dissociation group, it is expected that the C terminus of peptide **1** possesses a zwitterionic structure at pH 3.8, cationic charge at pH 2.2, and anionic charge at pH 6.4–11.6. Thus, it seems that the zwitterionic structure at the C terminus of peptide **1** is critical for the formation of viral-size monodispersed assemblies, with a cationic or anionic C terminus disturbing the assembly of peptide **1**. The pH dependence of self-assembly of peptide **1** is a contrast to that of 24-mer β-annulus peptide from TBSV, which form nanocapsules over a wide pH range (pH 2-13).[32]

CONCLUSIONS

We have demonstrated that a novel β-annulus peptide from SeMV bearing an FKFE sequence at the C terminus self-assembled into virus-like nanospheres. The size of the virus-like nanospheres was minimally affected by peptide concentration above CAC, but was drastically changed by pH. We propose that β-annulus motifs of various viruses modified by proper molecular design could be applied as building blocks for virus-like nanospheres. The present molecular design provides novel guidelines for the design of pH-responsive peptide nanospheres, which can be applied as drug carriers.

ACKNOWLEDGMENTS

This research was partially supported by The Canon Foundation and a Grant-in-Aid for Scientific Research (B) (No. 15H03838) from the Japan Society for the Promotion of Science (JSPS).

REFERENCES

1. Douglas, T.; Young, M. Science (2006), 312, 873–875.
2. Steinmetz, N. F.; Evans, D. J Org Biomol Chem (2007), 5, 2891–2902.
3. Bronstein, L. M. Small (2011), 7, 1609–1618.
4. Branden C.; Tooze, J. Introduction to Protein Structure, 2nd ed.; Garland Publishing;

New York, 1999.
5. Harrison S. C.; Kirschhausen, T.; Cell (1983), 33, 650–652.
6. Fotin, A.; Cheng, Y.; Sliz, P.; Grigorieff, N.; Harrison, S. C.; Kirchhausen, T.; Walz, T. Nature (2004), 432, 573–579.
7. Matsuura, K. RSC Adv (2014), 4, 2942–2953.
8. Ramakers, B. E. I.; van Hesta, J. C. M.; Löwik, D. W. P. M. Chem Soc Rev (2014), 43, 2743–2756.
9. Marsden, H. R.; Kros, A. Angew Chem Int Ed (2010), 49, 2988–3005.
10. Zhou, M.; Bentley, D.; Ghosh, I. J Am Chem Soc (2004), 126, 734–735.
11. Ryadnov, M. G.; Woolfson, D. N. Nat Mater (2003), 2, 329–332.
12. Ryadnov, M. G.; Woolfson, D. N. Angew Chem Int Ed (2003), 42, 3021–3023.
13. Boyle, A. L.; Bromley, E. H. C.; Bartlett, G. J.; Sessions, R. B.; Sharp, T. H.; Williams, C. L.; Curmi, P. M. G.; Forde, N. R.; Linke, H.; Woolfson, D. N. J Am Chem Soc (2012), 134, 15457–15467.
14. Hamley, I. W. Angew Chem Int Ed (2007), 46, 8128–8147.
15. Bowerman, C. J.; Nilsson, B. L. Biopolymers: Peptide Sci (2012), 98, 169–184.
16. Marini, D. M.; Hwang, W.; Lauffenburger, D. A.; Zhang, S.; Kamm, R. D. Nano Lett (2002), 2, 295–299.
17. Yokoi, H.; Kinoshita T.; Zhang, S. Proc Natl Acad Sci USA (2005), 102, 8414–8419.
18. Lim, Y.; Park, S.; Lee, E.; Jeong, H.; Ryu, J.-H.; Lee, M. S.; Lee, M. Biomacromolecules (2007), 8, 1404–1408.
19. Sawada, T.; Takahashi, T.; Mihara, H. J Am Chem Soc (2009), 131, 14434–14441.
20. Fletcher, J. M.; Harniman, R. L.; Barnes, Fr. R. H.; Boyle, A. L.; Collins, A.; Mantell, J.; Sharp, T. H.; Antognozzi, M.; Booth, P. J.; Linden, N.; Miles, M. J.; Sessions, R. B.; Verkade, P.; Woolfson, D. N. Science (2013), 340, 595–599.
21. Gradišar, H.; Božič, S.; Doles, T.; Vengust, D.; Hafner-Bratkovič, I.; Mertelj, A.; Webb, B.; Šali, A.; Klavžar S.; Jerala, R. Nat Chem Biol (2013), 9, 362–366.
22. Matsuura, K.; Murasato, K.; Kimizuka, N. J Am Chem Soc (2005), 127, 10148–10149.
23. Murasato, K.; Matsuura, K.; Kimizuka, N. Biomactromolecules (2008), 9, 913–918.
24. Matsuura, K.; Hayashi, H.; Murasato, K.; Kimizuka, N. Chem Commun (2011), 47, 265–267.
25. Matsuura, K. Polymer J (2012), 44, 469–474.
26. Matsuura, K.; Matsuyama, H.; Fukuda, T.; Teramoto, T.; Watanabe, K.; Murasato, K. Kimizuka, N. Soft Matter (2009), 5, 2463–2470.
27. Matsuura, K.; Tochio, K.; Watanabe, K.; Kimizuka, N. Chem Lett (2011), 40, 711–713.

28. Matsuura, K.; Fujino, K.; Teramoto, T.; Murasato, K.; Kimizuka, N. Bull Chem Soc Jpn (2010), 83, 880–886.
29. Olson, A. J.; Bricogne, G.; Harrison, S. C. J Mol Biol (1983), 171, 61–93.
30. Hopper, P.; Harrison, S. C.; Sauer, R. T. J Mol Biol (1984), 177, 701–713.
31. Matsuura, K.; Watanabe, K.; Sakurai, K.; Matsuzaki T.; Kimizuka, N. Angew Chem Int Ed (2010), 49, 9662–9665.
32. Matsuura, K.; Watanabe, K.; Matsushita, Y.; Kimizuka, N. Polymer. J. (2013), 45, 529–534.
33. Fujita, S.; Matsuura, K. Nanomaterials (2014), 4, 778–791.
34. Matsuura, K.; Ueno, G.; Fujita, S. Polymer. J. (2015), 47, 146–151.
35. Bhuvaneshwari, M.; Subramanya, H. S.; Gopinath, K.; Savithri, H. S.; Nayudu, M. V.; Murthy, M. R. N. Structure (1995), 3, 1021–1030.
36. Satheshkumar, P. S.; Lokesh, G. L.; Murthy, M. R.; Savithiri, H. S. J Mol Biol (2005), 353, 447–458.
37. Larson, S. B.; Day, J.; Canady, M. A.; Greenwood, A.; McPherson, A. J Mol Biol (2000), 301, 625–642.
38. Plevka, P.; Tars, K.; Zeltins, A.; Balke, I.; Truve, E.; Liljas, L. Virology (2007), 369, 364–374.
39. Katpally, U.; Kakani, K.; Reade, R.; Dryden, K.; Rochon, D.; Smith, T. J. J Mol Biol (2007), 365, 502–512.
40. Oda, Y.; Saeki, K.; Takahashi, Y.; Maeda, T.; Naitow, H.; Tsukihara, T.; Fukuyama, K. J Mol Biol (2000), 300, 153–169.
41. Powell, J. D.; Barbar, E.; Dreher, T. W. Virology (2012), 422, 165–173.

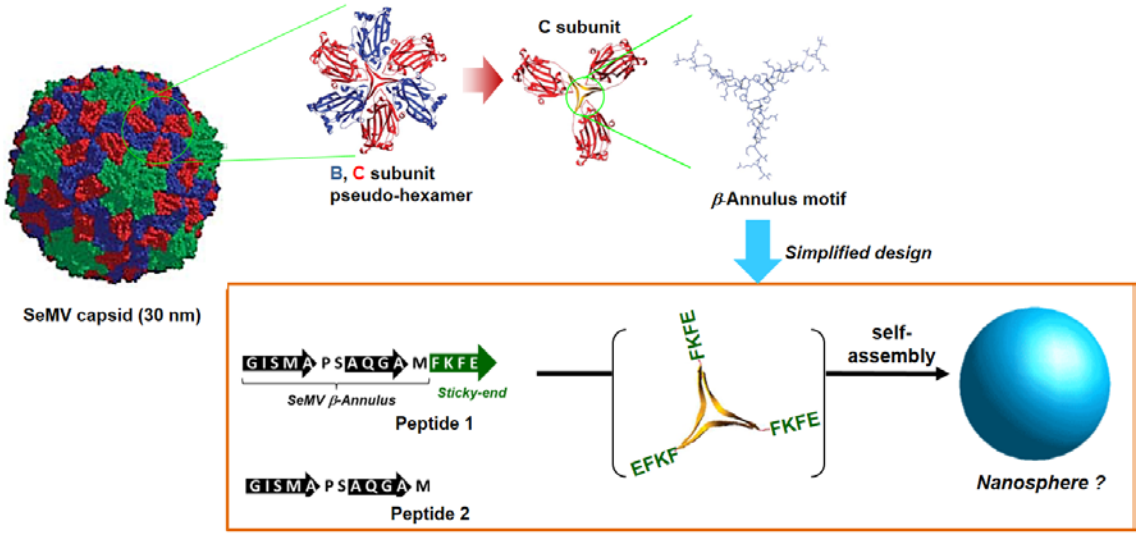

FIGURE 1 Schematic illustration of the hypothesized formation of a nanosphere through self-assembly of the modified *β*-annulus peptide of SeMV. Reproduced with permission from ref. 36. Copyright 2005, Elsevier.

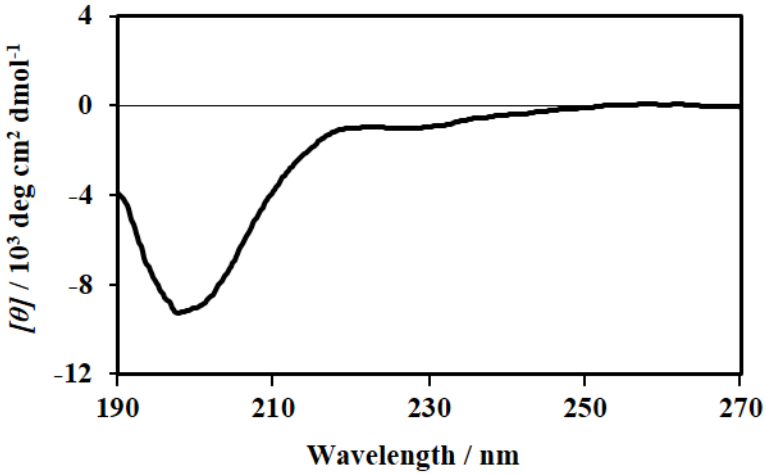

FIGURE 2 CD spectrum of an aqueous solution of peptide **1** (0.5 mM, pH 3.8) at 25 °C.

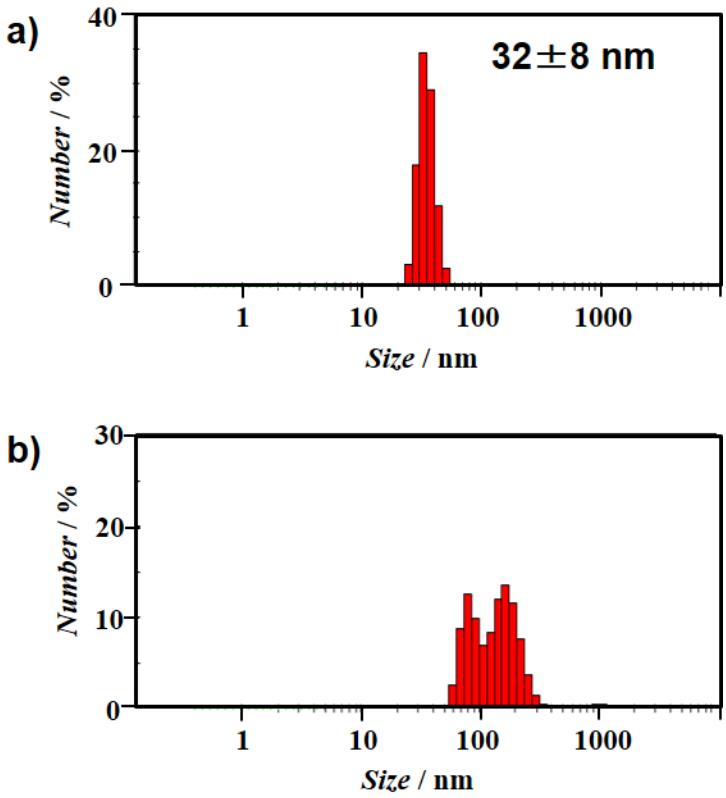

FIGURE 3 Size distribution of aqueous solutions of (a) peptide **1** (0.5 mM, pH 3.8) and (b) peptide **2** (0.1 mM containing 0.3% TFE) determined by DLS at 25 °C.

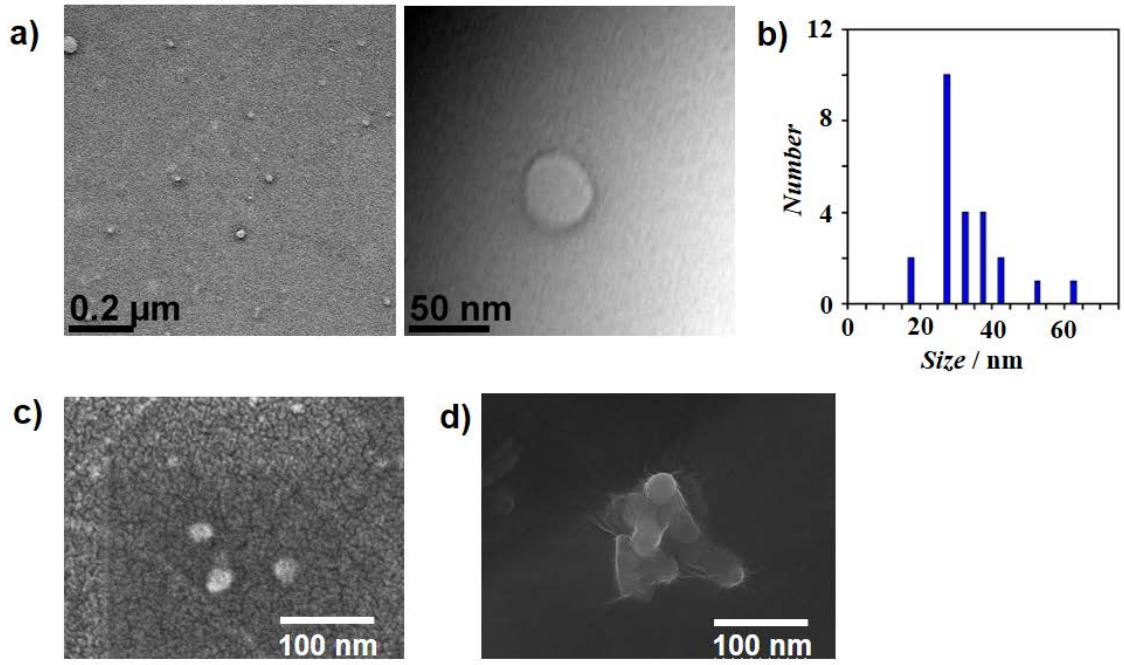

FIGURE 4 (a) TEM images of the assemblies obtained from an aqueous solution of peptide **1** (0.5 mM, pH 3.8) and (b) the size distribution determined from TEM. SEM images of the assemblies obtained from an aqueous solution of (c) peptide **1** (0.5 mM, pH 3.8) and (d) peptide **2** (0.1 mM containing 0.3% TFE).

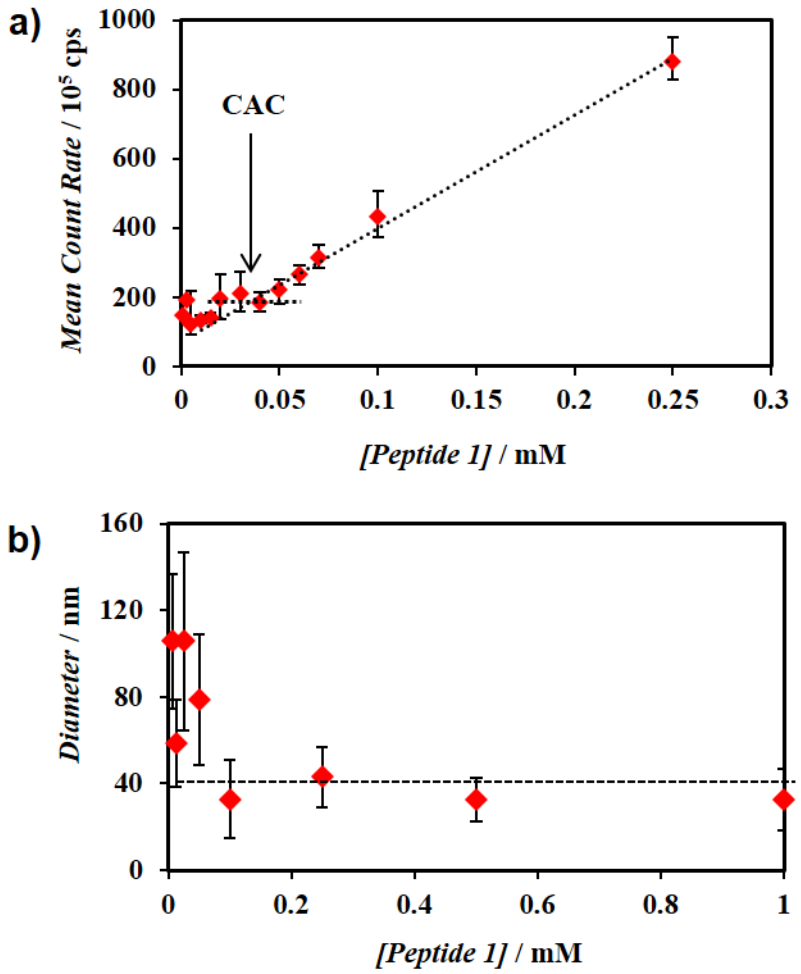

FIGURE 5 Effect of peptide concentration on scattering intensity (a) and size distribution (b) of an aqueous solution (pH 3.8) of peptide **1** determined by DLS at 25 °C.

pH 2.2

H_3N^+-GISMAPSAQGAMFK^+FE-COOH

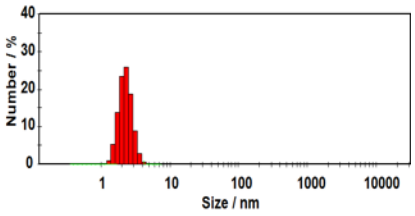

pH 3.8

H_3N^+-GISMAPSAQGAMFK^+FE-COO^-

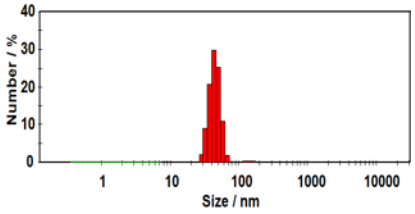

pH 6.4

H_3N^+-GISMAPSAQGAMFK^+FE^--COO^-

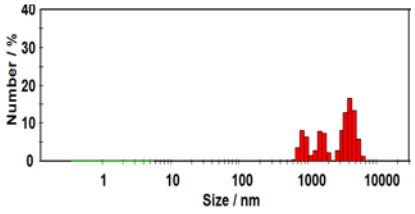

pH 8.2

H_3N^+-GISMAPSAQGAMFK^+FE^--COO^-

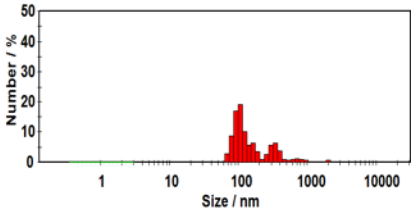

pH 11.6

H_2N-GISMAPSAQGAMFKFE^--COO^-

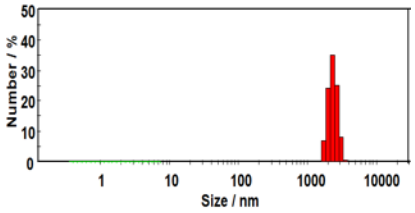

FIGURE 6 Effect of pH on the size distribution of an aqueous solution of peptide **1** (0.5 mM) determined by DLS at 25 °C.